



UNIVERSITY OF LEEDS

This is a repository copy of *Information theoretic measurement of blood flow complexity in vessels and aneurysms: Interlacing complexity index*.

White Rose Research Online URL for this paper:  
<http://eprints.whiterose.ac.uk/145302/>

Version: Accepted Version

---

**Proceedings Paper:**

Pozo, JM, Geers, AJ and Frangi, AF [orcid.org/0000-0002-2675-528X](https://orcid.org/0000-0002-2675-528X) (2017) Information theoretic measurement of blood flow complexity in vessels and aneurysms: Interlacing complexity index. In: Lecture Notes in Computer Science. International Conference on Medical Image Computing and Computer-Assisted Intervention: MICCAI 2017, 10-14 Sep 2017, Quebec, Canada. Springer Verlag , pp. 233-241. ISBN 9783319661841

[https://doi.org/10.1007/978-3-319-66185-8\\_27](https://doi.org/10.1007/978-3-319-66185-8_27)

---

© Springer International Publishing AG 2017. This is an author produced version of a conference paper published in Lecture Notes in Computer Science. Uploaded in accordance with the publisher's self-archiving policy.

**Reuse**

Items deposited in White Rose Research Online are protected by copyright, with all rights reserved unless indicated otherwise. They may be downloaded and/or printed for private study, or other acts as permitted by national copyright laws. The publisher or other rights holders may allow further reproduction and re-use of the full text version. This is indicated by the licence information on the White Rose Research Online record for the item.

**Takedown**

If you consider content in White Rose Research Online to be in breach of UK law, please notify us by emailing [eprints@whiterose.ac.uk](mailto:eprints@whiterose.ac.uk) including the URL of the record and the reason for the withdrawal request.



[eprints@whiterose.ac.uk](mailto:eprints@whiterose.ac.uk)  
<https://eprints.whiterose.ac.uk/>

# Information Theoretic Measurement of Blood Flow Complexity in Vessels and Aneurysms: Interlacing Complexity Index

Jose M. Pozo<sup>1</sup>, Arjan J. Geers<sup>2</sup>, and Alejandro F. Frangi<sup>1</sup>

<sup>1</sup> Center for Computational Imaging & Simulation Technologies in Biomedicine (CISTIB), Department of Electronic and Electrical Engineering, The University of Sheffield, Sheffield, UK.

<sup>2</sup> CISTIB, Department of Information and Communication Technologies, Universitat Pompeu Fabra, Barcelona, Spain

**Abstract.** Haemodynamics is believed to be a crucial factor in the aneurysm formation, evolution and eventual rupture. The 3D blood flow is typically derived by computational fluid dynamics (CFD) from patient-specific models obtained from angiographic images. Typical quantitative haemodynamic indices are local. Some qualitative classifications of global haemodynamic features have been proposed. However these classifications are subjective, depending on the operator visual inspection.

In this work we introduce an information theoretic measurement of the blood flow complexity, based on Shannon's Mutual Information, named Interlacing Complexity Index (ICI). ICI is an objective quantification of the flow complexity from aneurysm inlet to aneurysm outlets. It measures how unpredictable is the location of the streamlines at the outlets from knowing the location at the inlet, relative to the scale of observation.

We selected from the @neurIST database a set of 49 cerebral vasculatures with aneurysms in the middle cerebral artery. Surface models of patient-specific vascular geometries were obtained by geodesic active region segmentation and manual correction, and unsteady flow simulations were performed imposing physiological flow boundary conditions. The obtained ICI has been compared to several qualitative classifications performed by an expert, revealing high correlations.

**Keywords:** Aneurysms, CFD, haemodynamics, flow complexity, Mutual Information

## 1 Introduction

Aneurysms are pathologic dilations of the vessel wall. Prevalence of intracranial aneurysms (IA) is estimated to be between 2 and 5% [12] and their eventual rupture typically causes subarachnoid haemorrhage, resulting in high rates of morbidity and mortality. Different indicators of their natural evolution have been investigated based on diverse factors, including genetics, clinical conditions, aneurysm size and morphology, and aneurysm haemodynamics. Haemodynamics is believed to be a crucial factor in the aneurysm formation, evolution and

eventual rupture [9, 14]. For cerebral aneurysms, in vivo flow measurements with detailed resolution is unfeasible. Thus, the 3D blood flow is usually derived by computational fluid dynamics (CFD) from patient-specific models obtained by segmentation of angiographic images. From the time-varying blood flow field,  $\mathbf{v}(\mathbf{x}, t)$ , derived local quantities, such as wall shear stress, dynamic pressure and vorticity, are typically computed as local quantitative haemodynamic indices. For visualization purposes, also some loci are obtained, such as iso-velocity surfaces and streamlines. This allows to obtain a global qualitative impression or a subjective classification of the flow pattern, which has led to the definition of global haemodynamic indices such as flow pattern, flow complexity, flow stability, or recirculation zones. However, these indices are subjective, depending on operator visual inspection [4]. Objectively quantifying the flow complexity in IAs would eliminate the inter-observer variability and the need for flow visualization.

For general flows, complexity is related to the concept of chaos [19, 1], which has been studied from the perspective of dynamical systems and ergodic theory [7]. However, the derived flow complexity measures, such as Lyapunov exponents and Kolmogorov–Sinai entropy, are not feasible to study the aneurysmal flow. Whereas the blood flow transport through a vascular region of interest takes a finite time from inlet to outlet, those measures characterize flows infinitely propagated in time, or flows in periodic geometries [20, 5]. An alternative approach is focused in quantifying chaotic mixing [6, 16]. None of them is directly applicable to aneurysm since they consider the mixing of a two-phase fluid, or are only defined for flows in a closed container, without inlets and outlets.

Here, we introduce the *Interlacing Complexity Index* (ICI) as a measure of the complexity of a flow due to the chaotic mixing in the transport from inlet to outlet. This enables to apply it to the flow complexity quantification in aneurysms. ICI is inspired by communication theory [15], which deals with information flow as opposed to fluid flow. A communication system involves a transmitter, a receiver, and a communication channel. We can recognize parallel roles in those of, respectively, the inlet, the outlet, and the flow transport between them (Fig. 1). A position at the inlet (transmitted message) is connected by a flow streamline (channel) to a corresponding position at the outlet (received message), observed at a particular scale (noise). Shannon’s mutual information (MI) measures the amount of information effectively communicated. Thus, the more complex the flow, the lower the ability to discriminate the outlet position by knowing the inlet position, and the smaller the MI. The ICI is a function of the observation scale, defined as the normalization of this MI, so that  $ICI = 0$  for the simplest parallel flow and  $ICI \rightarrow 1$  for a very complex flow.

## 2 Interlacing Complexity Index

### 2.1 Natural Distribution of Streamlines

Let us consider any portion of the vascular system. Typically, it would have a tree structure. Thus, there would be one blood flow inlet and several outlets. But several inlets are also possible in the Circle of Willis. The flow at each instant  $t$  is

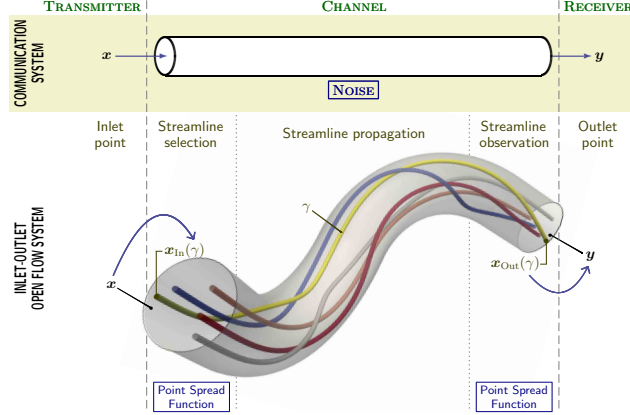


**Fig. 1.** Inlet-outlet flow system analogy to a communication system.

given by a vector field,  $\mathbf{v}(\mathbf{x})$ , representing the local fluid speed. The *congruence of streamlines*,  $\Gamma$ , at one instant is the set of lines generated by integrating this vector field. We can then assign to each streamline,  $\gamma$ , its Cartesian coordinates when crossing the inlet,  $\mathbf{x}_{\text{In}}(\gamma)$ , or the outlet,  $\mathbf{x}_{\text{Out}}(\gamma)$ . We define the *natural distribution of streamlines* as the one given by the probability density

$$p(\mathbf{x}_{\text{In}}) = \frac{\mathbf{v}(\mathbf{x}_{\text{In}}) \cdot \hat{\mathbf{n}}(\mathbf{x}_{\text{In}})}{\int_{\text{In}} \mathbf{v}(\mathbf{x}_{\text{In}}) \cdot \hat{\mathbf{n}}(\mathbf{x}_{\text{In}}) d\mathbf{x}_{\text{In}}} \quad (1)$$

or the corresponding expression for the outlet. Here  $\hat{\mathbf{n}}$  denotes the normal vector at any point of the inlet or the outlet. For incompressible flows, the obtained distribution of streamlines (denoted symbolically by  $p(\gamma)$ ) is invariant to it being generated at the inlet or the outlet.

## 2.2 Scale-Dependent Mutual Information

To compute the MI between location at inlet,  $\mathbf{x}_{\text{In}}$ , and outlet,  $\mathbf{x}_{\text{Out}}$ , connected by the same streamline, we must define their joint probability distribution,  $p(\mathbf{x}_{\text{In}}, \mathbf{x}_{\text{Out}})$ . For an infinite-precision localization of points, this would produce Dirac deltas, which will result in infinite MI. Thus, we introduce a scale of observation,  $s$ , and a corresponding Gaussian point spread function (PSF) defining conditional probability densities at the inlet,  $p_s(\mathbf{x}_{\text{In}} | \gamma)$ , and outlet,  $p_s(\mathbf{x}_{\text{Out}} | \gamma)$ , with standard deviations proportional to the area-equivalent radius,  $\sigma = sR$ , of inlet and outlet, respectively. This provides the joint probability density

$$p_s(\mathbf{x}_{\text{In}}, \mathbf{x}_{\text{Out}}) = \int_{\Gamma} p_s(\mathbf{x}_{\text{In}} | \gamma) p_s(\mathbf{x}_{\text{Out}} | \gamma) p(\gamma) d\gamma . \quad (2)$$

From this we can compute the MI

$$I_s = \int_{\text{Inlet}} d\mathbf{x}_{\text{In}} \int_{\text{Outlet}} d\mathbf{x}_{\text{Out}} p_s(\mathbf{x}_{\text{In}}, \mathbf{x}_{\text{Out}}) \log \left( \frac{p_s(\mathbf{x}_{\text{In}}, \mathbf{x}_{\text{Out}})}{p_s(\mathbf{x}_{\text{In}}) p_s(\mathbf{x}_{\text{Out}})} \right) , \quad (3)$$

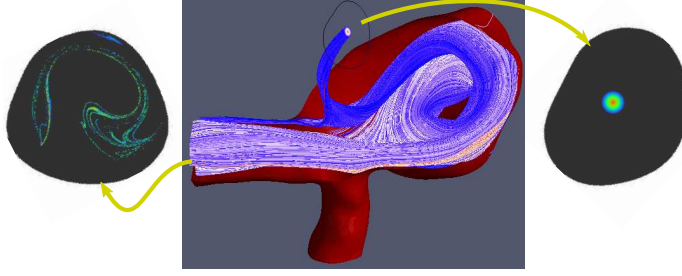


**Fig. 2.** Example of a subset of streamlines around one outlet point and their corresponding points at the inlet, displaying an elongated and complex pattern.

which is a function of the scale  $s$ .

### 2.3 Interlacing Complexity Index

The ICI is defined as a normalized distance based on MI, analogous to  $d_{\max} = 1 - NMI_{\max}$  for discrete variables [8]:

$$ICI_s = 1 - \frac{I_s}{\max\{I_s^{(\text{In})}, I_s^{(\text{Out})}\}}. \quad (4)$$

Here, the inlet self MI,  $I_s^{(\text{In})}$ , is the MI corresponding to the probability density

$$p_s(\mathbf{x}_{\text{In}}, \mathbf{x}'_{\text{In}}) = \int_{\Gamma} p_s(\mathbf{x}_{\text{In}} | \gamma) p_s(\mathbf{x}'_{\text{In}} | \gamma) p(\gamma) d\gamma, \quad (5)$$

and analogously for the outlet  $I_s^{(\text{Out})}$ . Thus, ICI is expected to be in the range  $[0, 1]$ , with  $ICI_s = 0$  for a perfectly laminar parallel flow, and  $ICI_s \rightarrow 1$  for a very complex flow.

## 3 Numerical Estimation of ICI in Aneurysms

### 3.1 Blood Flow Simulation from Patient-Specific Vasculatures

3D Rotational Angiography (3DRA) images of the cerebral vasculature from 49 patients including an aneurysm in the Middle Cerebral Artery (MCA) have been selected from the @neurist database [17]. A surface model of the patient-specific vascular geometry is obtained with the Geometric Active Region (GAR) segmentation [2] and manually corrected using the suite @neufuse [17]. The vasculature of interest includes at least 12 vessel diameters upstream and 4 vessel diameters downstream from the aneurysm, clipped with planes perpendicular to the vessel centerline. Unstructured volumetric meshes have been created using an octree approach with ICM CFD 13.0 (ANSYS, Canonsburg, PA, USA),

composed of tetrahedral elements with side length 0.24 mm and three layers of prism elements at the wall with total height of 0.08 mm and side length 0.12 mm. Unsteady flow simulations have been performed with CFX 13.0 (ANSYS) for incompressible Newtonian fluid with viscosity  $\mu = 3.5 \text{ mPa s}$  and density  $\rho = 1066 \text{ kg m}^{-3}$  (typical values for blood) and imposing rigid walls and flow rate (inlet) and pressure waveforms (outlets) extracted from a one-dimensional model of all the large arteries in the human body [11], for a cardiac cycle of period 0.8 s.

### 3.2 Inlet and Outlet Selection

To evaluate the complexity introduced in the blood flow due to the presence of the aneurysm, inlet and outlets have been automatically selected as cross-sections perpendicular to the vessel centerline at around one vessel diameter from the aneurysm neck, following the same criterion introduced in [10].

### 3.3 Streamlines Generation and ICI Estimation

The streamlines at two physiologically relevant cardiac phases: peak systole (PS) and end diastole (ED), have been integrated from the flow velocity field using 4th order Runge–Kutta algorithm, implemented in the Visualization ToolKit library [18]. Congruences of  $N$  streamlines have been generated by selecting  $N$  seed points according to the natural distribution (1).

The integrations (3) required for  $I_s$ ,  $I_s^{\text{In}}$ , and  $I_s^{\text{Out}}$  have been computed by Monte Carlo [13], using uniform samplings of  $M$  points in both the inlet and the outlet. From them,  $ICI_s$  was computed as defined by (4).

## 4 Experiments

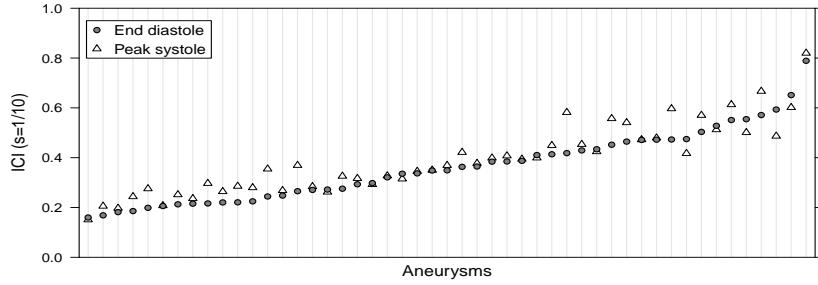
### 4.1 Algorithm Accuracy and Precision Evaluation

To estimate the algorithm precision and accuracy we have selected a random subset of 10 aneurysms, considering their  $ICI_s$  at peak systole. We have considered as ground-truth, the values obtained with  $N = 100\text{k}$  streamlines and  $M = 50\text{k}$  points, which is in the limit of the feasible computation.  $ICI_s$  has been also computed for  $N = 5\text{k}, 10\text{k}, 20\text{k}, 50\text{k}$  and  $M = 2\text{k}, 5\text{k}, 10\text{k}, 20\text{k}$ , instantiated twice for each combination. For each scale, the signed error is given by the difference with respect to the ground truth,  $\varepsilon_s = ICI_s - ICI_s^{(\text{GT})}$ . Table 1 presents the estimated accuracy and precision for 3 different settings for  $N$  and  $M$ , where the accuracy is quantified by the mean signed error,  $\bar{\varepsilon}$ , and the precision by twice its standard deviation,  $2\sigma_{\varepsilon}$ , representing approximately the 95% confidence interval ( $\bar{\varepsilon} \pm 2\sigma_{\varepsilon}$ ).

Both accuracy and precision increase with the number of streamlines ( $N$ ) and with the number of points ( $M$ ). From the obtained values, a reasonable selection seems to be  $N = 20\text{k}$  and  $M = 5\text{k}$ , involving an acceptable mean computational time of 5 minutes per case.

**Table 1.** Accuracy ( $\bar{\varepsilon}$ ) and precision ( $2\sigma_\varepsilon$ ) of  $ICI_s$  for 3 scales and 3 settings of  $N$  and  $M$ . The values are expressed as  $\bar{\varepsilon} \pm 2\sigma_\varepsilon$  (approximate 95% confidence interval).

	$N = 5k, M = 2k$	$N = 20k, M = 5k$	$N = 50k, M = 20k$
$s = 1/3$	$0.001 \pm 0.032$	$0.002 \pm 0.012$	$0.001 \pm 0.008$
$s = 1/10$	$-0.005 \pm 0.010$	$0.000 \pm 0.006$	$0.000 \pm 0.003$
$s = 1/20$	$-0.018 \pm 0.022$	$-0.003 \pm 0.007$	$-0.001 \pm 0.003$

**Fig. 3.** Distribution of ICI across MCA aneurysms at PS and ED.

## 4.2 Distribution of ICI in the Population of Aneurysms

The values of  $ICI_{1/10}$  across the sample of aneurysms at PS and ED are displayed in Fig. 3. The values spread quite homogeneously across the ICI range, and the complexity at PS and ED are clearly separated for most cases. This result evidences that ICI is a sensitive measurement of flow complexity in aneurysms. In general, the ICI obtained for PS is larger than the one obtained for ED, but the opposite behaviour is also observed.

## 4.3 Comparison with Subjective Flow Complexity and Stability

For each aneurysm, the flow field has been qualitatively assessed by an expert, through visual inspection of the streamlines, according to 2 qualitative variables [3, 4]: flow complexity (*simple* or *complex*), assessed at PS, and flow stability (*stable* or *unstable*) assessed by comparing the flow patterns at PS and ED.

We have investigated the correlation of the proposed quantitative ICI with these subjective qualitative classifications. Fig. 4 shows a box-plot of  $ICI_{1/10}$  at PS compared to flow complexity and a box-plot of the absolute value of the difference between  $ICI_{1/10}$  at PS and ED compared to flow stability. The classes are not exactly recovered, since some overlap is observed, but highly statistically significant differences were obtained with the non-parametric Mann–Whitney  $U$  test (flow complexity:  $p = 9 \times 10^{-3}$ ; flow stability:  $p = 5 \times 10^{-4}$ ). This result supports that ICI is related with these subjective classifications, providing a meaningful biomarker.

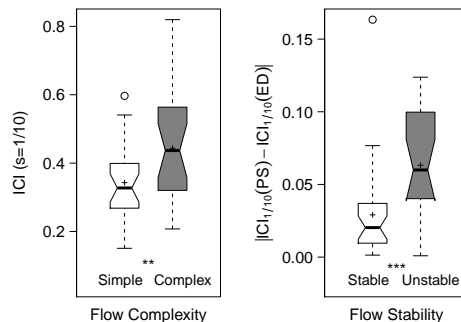


**Fig. 4.** Correlation of ICI with the subjective flow classifications. The significant difference between each pair of categories is assessed by non-parametric Mann–Whitney  $U$  test. \*\* ( $p < 0.01$ ), \*\*\* ( $p < 0.001$ ).

## 5 Conclusions

In this paper, we have introduced the interlacing complexity index (ICI), inspired in information theory, as an objective measure of the flow complexity for vasculatures with aneurysms. The behaviour of ICI has been tested with numerical experiment on a dataset of MCA aneurysms. The estimation of ICI from finite samples of streamlines has shown good accuracy and precision. The results indicate that ICI provides a sensitive flow complexity measure, discriminating across the population of aneurysm and between ED and PS, with an intuitive interpretation, and in agreement with subjective classifications. This supports the potential of ICI as biomarker for the natural evolution of aneurysms, and to quantify differences in follow-ups and between treatment options. For instance ICI could quantify how aneurysm growth or flow diverter treatment affects flow complexity.

ICI has been compared with subjective classifications, which inherently entails some variability and can be affected by the visualization of only a limited number of streamlines. In its turn, ICI can be affected by the pre-processing steps for flow simulation. These relevant factors will be considered in subsequent studies.

## References

1. Aref, H., Blake, J.R., Budišić, M., Cartwright, J.H.E., Clercx, H.J.H., Feudel, U., Golestanian, R., Guillard, E., Guer, Y.L., van Heijst, G.F., et al.: Frontiers of chaotic advection. arXiv preprint arXiv:1403.2953 (2014)
2. Bogunović, H., Pozo, J.M., Villa-Uriol, M.C., Majoie, C.B.L.M., van den Berg, R., Gratama van Andel, H.A.F., Macho, J.M., Blasco, J., San Román, L., Frangi, A.F.: Automated segmentation of cerebral vasculature with aneurysms in 3DRA

- and TOF-MRA using geodesic active regions: An evaluation study. *Med Phys* 38, 210 (2011)
3. Cebal, J.R., Mut, F., Weir, J., Putman, C.M.: Association of hemodynamic characteristics and cerebral aneurysm rupture. *Am J Neuroradiol* 32(2), 264–270 (2011)
  4. Geers, A.J., Larrabide, I., Radaelli, A.G., Bogunovic, H., Kim, M., van Andel, H.A.F.G., Majoie, C.B., VanBavel, E., Frangi, A.F.: Patient-specific computational hemodynamics of intracranial aneurysms from 3D rotational angiography and CT angiography: an in vivo reproducibility study. *Am J Neuroradiol* 32(3), 581–586 (2011)
  5. Jang, B., Funakoshi, M.: Chaotic mixing in a helix-like pipe with periodic variations in curvature and torsion. *Fluid Dyn Res* 42(3), 035506 (2010)
  6. Lin, Z., Thiffeault, J.L., Doering, C.R.: Optimal stirring strategies for passive scalar mixing. *J Fluid Mech* 675, 465–476 (2011)
  7. Mathew, G., Mezić, I.: Metrics for ergodicity and design of ergodic dynamics for multi-agent systems. *Physica D* 240(4), 432–442 (2011)
  8. McDaid, A.F., Greene, D., Hurley, N.: Normalized mutual information to evaluate overlapping community finding algorithms. arXiv preprint arXiv:1110.2515 (2011)
  9. Meng, H., Tutino, V., Xiang, J., Siddiqui, A.: High WSS or low WSS? Complex interactions of hemodynamics with intracranial aneurysm initiation, growth, and rupture: toward a unifying hypothesis. *Am J Neuroradiol* 35(7), 1254–1262 (2014)
  10. Millan, R.D., Dempere-Marco, L., Pozo, J.M., Cebal, J.R., Frangi, A.F.: Morphological characterization of intracranial aneurysms using 3-D moment invariants. *IEEE Trans Med Imag* 26(9), 1270–1282 (Sept 2007)
  11. Reymond, P., Merenda, F., Perren, F., Rüfenacht, D., Stergiopulos, N.: Validation of a one-dimensional model of the systemic arterial tree. *Am J Physiol-Heart C* 297(1), H208–H222 (2009)
  12. Rinkel, G.J.E., Djibuti, M., Algra, A., Van Gijn, J.: Prevalence and risk of rupture of intracranial aneurysms a systematic review. *Stroke* 29(1), 251–256 (1998)
  13. Robert, C., Casella, G.: Monte Carlo Statistical Methods. Springer Science & Business Media (2013)
  14. Sforza, D.M., Kono, K., Tateshima, S., Viñuela, F., Putman, C., Cebal, J.R.: Hemodynamics in growing and stable cerebral aneurysms. *J Neurointerv Surg* 8(4), 407–412 (2016)
  15. Shannon, C.E., Weaver, W.: The Mathematical Theory of Information. Univ. of Illinois Press, Urbana, Illinois (1949)
  16. Thiffeault, J.L.: Using multiscale norms to quantify mixing and transport. *Nonlinearity* 25(2), R1 (2012), <http://stacks.iop.org/0951-7715/25/i=2/a=R1>
  17. Villa-Uriol, M.C., Berti, G., Hose, D.R., Marzo, A., Chiarini, A., Penrose, J., Pozo, J.M., Schmidt, J.G., Singh, P., Lycett, R., Larrabide, I., Frangi, A.F.: @neurist complex information processing toolchain for the integrated management of cerebral aneurysms. *Interface Focus* 1(3), 308–319 (2011)
  18. VTK community: VTK visualization toolkit. <http://www.vtk.org> (2014)
  19. Wiggins, S., Ottino, J.M.: Foundations of chaotic mixing. *Phil Trans R Soc A* 362(1818), 937–970 (2004)
  20. Xia, H.M., Shu, C., Chew, Y.T., Wang, Z.P.: Approximate mapping method for prediction of chaotic mixing in spatial-periodic microchannel. *Chem Eng Res Des* 88(10), 1419–1426 (2010)